13

Probing Protein–Protein Interactions with Mass Spectrometry

Richard W. Kriwacki and Gary Siuzdak

1. Introduction

Protease mapping is an established method for probing the primary structure of proteins ***(1,2)*** and has traditionally been performed through the use of chromatography and/or gel electrophoresis techniques in combination with Edman degradation NH_2-terminal sequencing ***(3)***. More recently, mass spectrometry has been combined with protease mapping to perform "protein mass mapping." Definitively, protein mass mapping combines enzymatic digestion, mass spectrometry, and computer-facilitated data analysis to examine proteolytic fragments for protein structure determination. Protein mass mapping permits the identification of protein primary structure by applying sequence-specific proteases and performing mass analysis on the resulting proteolytic fragments, thus yielding information on fragment masses with accuracy approaching ±5 ppm, or ±0.005 Daltons for a 1000 Daltons peptide. The protease fragmentation pattern is then compared with the patterns predicted for all proteins within a database, and matches are statistically evaluated. Since the occurrence of Arg and Lys residues in proteins is statistically high, trypsin cleavage (specific for Arg and Lys) generally produces a large number of fragments, which, in turn, offer a reasonable probability for unambiguously identifying the target protein. The success of this strategy relies on the existence of the protein sequence within the database, but with the sequences of whole genomes for several organisms now complete (*Escherichia coli*, *Bacillus subtilis*, and *Archaeoglobus fulgidus*) and others approaching completion (*Saccharomyces cerevisiae*, *Saccaramyces pombe*, *Homo sapiens*, and so forth), the likelihood for matches is reasonably high. Although exact matches are

From: *Methods in Molecular Biology, vol. 146:*
Protein and Peptide Analysis: New Mass Spectrometric Applications
Edited by: J. R. Chapman

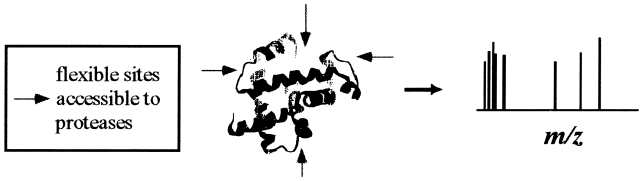

Fig. 1. Illustration of the use of proteolytic cleavage as a probe of protein structure. The arrows mark surface-exposed and flexible sites that would be susceptible to proteolytic cleavage. If a sequence-specific protease were used, the marked sites would also have to contain the protease recognition sequence to sustain cleavage. Mass analysis of all fragments together yields the cleavage "map" that provides information on secondary and tertiary structure.

readily identified, homologous proteins are also identified (albeit with lower statistical significance), whereby a target protein is placed within a particular family in the absence of an exact match.

The basis for studying tertiary structure using protein mass mapping is the application of limited proteolytic digestion with mass spectrometry ***(4,5)***. In the analysis of protein structure, a factor that governs the selectivity of cleavage is the sequence specificity of the enzyme. A sequence-specific protease reduces the number of fragments that are produced and, concomitantly, improves the likelihood of statistically significant matches between observed and predicted fragment masses and reduces the opportunities for spurious matches. Another factor, the accessibility/flexibility of the site to the protease ***(6,7)*** also plays an important role in the analysis of structure where, ideally, only a subset of all possible cleavages are observed due to the inaccessibility of some sites due to higher order protein structure. An example of this can be seen in **Fig. 1**, where arrows mark potential cleavage sites within a hypothetical protein; these sites are surface exposed and located in flexible loop regions. The distribution of amino acids in a protein guides the choice of protease to be used as a structural probe. Since amino acids with hydrophilic side chains are found in greater abundance on the surface of proteins (at the solvent interface), proteases that cleave at hydrophilic sites are preferred in structural analysis. Trypsin and V8 protease, which cleave basic (K, R) and acidic (D, E) sites, respectively, are good choices. In addition, non-sequence-specific proteases such as subtilisin Carlsberg are often used as structural probes.

Fig. 1

Protein mass mapping can also be used to probe the quaternary structure of multicomponent assemblies, including protein-protein complexes ***(4,5)*** and protein-DNA complexes ***(8)***. A common feature of these applications is that the protease is used to provide contrast between the associated and unassociated states of the system. The formation of an interface between a protein and another

macromolecule will exclude both solvent molecules and macromolecules such as proteases and will also protect otherwise accessible sites from protease cleavage. Methods developed for primary sequence elucidation using mass spectrometry are particularly well suited to the analysis of higher order, native protein structure since they are directly transferable to the analysis of native structure. Analysis methods, however, must be modified to take into account the added spectral complexity due to incomplete proteolysis under limiting conditions.

1.1. Analysis of Protein–DNA Interactions

The first application of limited proteolysis and matrix-assisted laser desorption/ionization (MALDI) mass spectrometry to the study of a multicomponent biomolecular assembly was published by Chait and co-workers in 1995 ***(8)***. This combined approach was used for the structural analysis of the protein transcription factor Max, both free in solution and bound to an oligonucleotide containing its specific DNA binding site. Max is a member of the basic helix-loop-helix (bHLH) family of DNA binding proteins and has also been the target of crystallographic studies. An extensive series of limited proteolysis experiments by Chait was conducted using free Max. The products of digestion reactions were analyzed using MALDI time-of-flight mass spectrometry (TOF-MS), demonstrating the suitability of this mass spectrometric technique in the analysis of multicomponent biomolecular samples, both for identification of fragments and for their relative quantitation. The results showed that Max is generally very susceptible to proteolytic cleavage. However, Max is less susceptible to digestion by a variety of proteases at high ionic strength, indicating that salt stabilizes Max structure. Since cleavage requires both accessibility and flexibility, this result suggested that Max structure is more highly ordered in the presence of higher salt concentrations, with loop regions in less flexible states. These results, indicating that Max may be relatively flexible in the absence of DNA, are consistent with the inability to crystallize Max in the free state. Much more dramatic stabilization of Max was observed in the presence of specific DNA. In this case, cleavage rates were reduced 100-fold, indicating that the Max protein is significantly stabilized in the presence of DNA. This stabilization stems partly from the protection of potential cleavage sites on formation of the Max-DNA interface and partly from the added thermodynamic stability imparted to Max by association with DNA. The cleavage pattern within the Max-DNA complex revealed that the bHLH domain is the minimal requirement for DNA binding and, importantly, that the leucine-zipper domain is dispensable for this activity. Furthermore, the locations of the Max-DNA interaction sites were identified. These results provided valuable insights into Max-DNA binding and the structure-function relationships

that guided the successful crystallization and structure determination of the Max-DNA complex.

The following describes the application of the approach outlined above to protein-protein interactions, specifically its use to probe the solution structure of a protein-protein complex between cell cycle regulatory proteins, p21 and Cdk2. Analysis of proteolytic digests of the p21-Cdk2 complex revealed a segment of between 22 and 36 amino acids of p21 that is protected from trypsin cleavage, identifying this as the Cdk2 binding site on p21. This approach was further utilized for the protein-protein complexes on viral capsids, including those of the common cold virus where, in addition to structural information, protein mass mapping revealed mobile features of the viral proteins.

2. Materials

2.1. Protein Preparation

1. Expression vector, pET-24a (Novagen, Madison, WI).
2. *Drosophila* cells (Schneider's line 1).
3. Schneider's insect medium.
4. Fetal bovine serum (Atlanta Biologicals, Norcross, GA).

2.2. Labeled Reagents

1. ^{15}N-labeled ammonium chloride (Martek, Columbia, MD).

2.3. Protein Chromatography

1. Ni^{2+}-affinity chromatography (Chelating sepharose, Amersham Pharmacia Biotech, Piscataway, NJ).
2. Anion-exchange chromatography (Q-sepharose, Amersham Pharmacia).
3. Reversed-phase high-performance liquid chromatography (HPLC; C4, Vydac, Hesperia, CA).

2.4. Proteases

1. Trypsin, clostripain (Arg-C), V8 protease (Glu-C), and Lys-C (Promega, Madison, WI).
2. Asp-N (Calbiochem, La Jolla, CA).
3. Carboxypeptidase Y [CPY] (Sigma).

2.5. Buffers

1. Tris-HCl, Tris (pH 7.5).
2. 0.1 *M* HEPES (pH 7.0).

2.6. General Reagents and Solvents

Phenylmethylsulfonyl fluoride (PMSF), trichloroacetic acid (TCA), 2-mercaptoethanol, sucrose, trifluoroacetic acid (TFA), ethylenediamine tetraacetic

acid (EDTA), BSA, $CaCl_2$, tosyllysine chloromethyl ketone (TLCK), NaCl, dithiothreitol (DTT), Nonidet p-40, and CH_3CN.

2.7. MALDI Matrices

2,5-Dihydroxybenzoic acid, 3,5-dimethoxy-4-hydroxycinnamic acid (Aldrich).

2.8. Instrumentation

1. PerSeptive Voyager Elite MALDI-MS with delayed extraction and nitrogen laser.
2. Kratos MALDI-IV MALDI-MS with delayed extraction and nitrogen laser.
3. Mass spectrometer sample plate derivatized with trypsin (Intrinsic Bioprobes [Tempe, AZ]).

2.9. Data Processing

1. Protein Analysis Worksheet (PAWS, Macintosh version 6.0b2, copyright © 1995, Dr. Ronald Beavis) available on the Internet.

3. Methods and Discussion

3.1. p21-B, ^{15}N-p21-B, and p21-B/Cdk2 Complex Experiments

p21-B was overexpressed in *E. coli* after the insertion of the gene segment for amino acids 9–84 of p21 plus an N-terminal (His)6 purification tag into the expression vector, pET-24a ***(9)***. ^{15}N-labeled p21-B was prepared using a "minimal media" recipe based on that originally developed by Neidhardt et al. ***(10)*** using ^{15}N-labeled ammonium chloride. Cdk2 was obtained after overexpression in Sf9 insect cells using a bacculovirus provided by Dr. David Morgan ***(11)*** and was kindly provided by Drs. Mark Watson and Steve Reed.

3.1.1. Purification and Preparation of p21-B and ^{15}N-p21-B

1. Purify p21-B or ^{15}N-p21-B in three steps:
   a. Ni^{2+}-affinity chromatography using chelating sepharose (Amersham Pharmacia Biotech).
   b. Anion-exchange chromatography using Q-sepharose (Amersham Pharmacia).
   c. Reversed-phase HPLC using a C4 column (Vydac).
2. Prepare p21-B solutions for proteolysis/MALDI-MS experiments by dissolving lyophilized material in distilled water at 1 mg/mL. Dilute this solution 1:10 (vol/vol) into 50 m*M* Tris (pH 7.5), 500 m*M* NaCl, 1 m*M* DTT, and 1 m*M* EDTA.

3.1.2. Preparation of p21-B/Cdk2 and ^{15}N-p21-B/Cdk2 Complexes

1. Prepare the p21-B/Cdk2 or ^{15}N-p21-B/Cdk2 complex by adding a highly concentrated Cdk2 solution (≈ 300 μ*M*) to the appropriate p21-B solution to achieve a final concentration of 20 μ*M* for each component.

3.1.3. Proteolysis of Free p21-B and p21-B/Cdk2 and ^{15}N-p21-B/Cdk2 Complexes

1. Mix a 20–60-μ*M* solution of free p21-B or of the complex, prepared as in **Subheading 3.1.2.** above, together with trypsin to give a protein-to-trypsin ratio of 1000:1–50:1 (mass/mass). Also, 50 m*M* Tris (pH 7.5), 500 m*M* NaCl, 10 m*M* DTT, and 1 m*M* EDTA are present, as detailed in **Subheading 3.1.1.**
2. Carry out proteolysis at 23°C for 30 min and then follow with the addition of PMSF to 1 m*M* and TCA to 10% (wt/vol).
3. Recover protein fragments by centrifugation and then dissolve in 50/50 CH_3CN/H_2O with 0.1% TFA for MALDI-MS analysis.

3.1.4. MALDI Mass Measurements of Proteolysis Products

1. Combine digest samples (40 μ*M*) with 2,5-dihydroxybenzoic acid matrix (≈ 0.2 *M* in 50%/50%/0.5% H_2O/CH_3CN/TFA) at a 1:1 volume ratio.
2. Deposit 2 μL of the sample-matrix mixture onto the MALDI instrument (PerSeptive Voyager Elite MALDI-MS) solution sample plate and insert into the ionization source.
3. Irradiate samples with a nitrogen laser (Laser Science [Franklin, MA]) operated at 337 nm (*see* **Note 1**).

3.2. Flock House and Human Rhinovirus Experiments

3.2.1. Preparation of FHV and HRV14

Flock House virus (FHV) was prepared in *Drosophila* cells (Schneider's line 1) suspended to 4×10^7 cells/mL in a complete growth medium containing Schneider's insect medium with 15% fetal bovine serum (CGM). FHV was added at a multiplicity of 120 plaque-forming units/cell and allowed to attach for 1 h at 26°C. HRV14 was prepared as previously described (*see* **Note 2**) to a final concentration of 1 mg/mL in 10 m*M* Tris buffer at pH 7.6.

1. Sediment cells and then resuspend them to 5 × 106 cells/mL in CGM.
2. Distribute aliquots onto 100-mm tissue culture plates and incubate at 26°C.
3. Remove the medium at 15 h post infection and rinse monolayers with 10 mL of ice-cold HE buffer (0.1 *M* HEPES, pH 7.0, 10 m*M* EDTA, 0.1% 2-mercaptoethanol, 0.1% BSA).
4. Lyse cells in 2 mL of ice-cold HE buffer containing 1% (v/v) Nonidet p-40.
5. Remove nuclei and cell debris from the lysate by centrifugation for 5 min at 4°C in a table-top centrifuge. Pellet the supernatant containing the virus through 2-mL sucrose gradients [10–30% (w/w) in HE buffer without BSA] at 100,000 rpm for 13 min.
6. Resuspend the pellets in 400 μL 5 m*M* $CaCl_2$ containing 0.1% 2-mercaptoethanol and buffered with HEPES (pH 7.0).

AU: pls. convert rpm to *g* force

3.2.2. Proteolytic Digests of FHV

1. Set up proteolytic digests at 25°C and 1 mg/mL virus using clostripain (Arg-C), V8 protease (Glu-C), Lys-C, or Asp-N in the manufacturer's recommended reaction buffer or trypsin in 25 m*M* Tris-HCl (pH 7.7) containing 1 m*M* EDTA (*see* **Note 3**).
2. Adjust enzyme-to-virus ratio (w/w) to 1:3000 in a total volume of 10–20 μL to achieve time-resolved cleavage.
3. Withdraw 0.5 μL from the digest at each time point beginning with a sampling rate of one per minute over a period of 1 min to 24 h.
4. Place the 0.5 μL reaction volume directly on the MALDI analysis plate and allow it to dry before the addition of matrix (*see* **Subheading 3.2.4.**).

To confirm the identity of trypsin-released fragments, the digest was further exposed to the exoprotease carboxypeptidase Y (CPY) to obtain C-terminal sequence information on each of the trypsin fragments as follows.

1. Inhibit the trypsin digest sample (**step 4** above) by the addition of TLCK 50 μg/mL and allow the mixture to dry on the MALDI sample plate.
2. Add CPY (1–3 μL of enzyme diluted to 1 mg/mL in water) to the dried trypsin digest and allow digestion to continue at room temperature until stopped by evaporation.

3.2.3. Proteolytic Digests of HRV14

1. Set up trypsin digest at 25°C with 1 mg/mL virus in 25 m*M* Tris HCl (pH 7.7).
2. Adjust the enzyme-to-virus ratio to 1:100 (w/w) in a total reaction volume of 10 μL.
3. Remove 0.50 μL samples from the reaction at each time point (5, 10, and 60 min), place directly on the MALDI analysis plate, and allow to dry before the addition of matrix (*see* **Subheading 3.2.4.**).
4. Alternatively, carry out on-plate digestions (data not shown) at room temperature using a mass spectrometer sample plate previously derivatized with trypsin.

3.2.4. Mass Spectrometry of Proteolytic Digests

1. Add MALDI matrix (0.5 μL of 3,5-dimethoxy-4-hydroxycinnamic acid in a saturated solution of acetonitrile/water (50:50) containing 0.25% TFA) to the dried sample on the instrument (PerSeptive Biosystems Voyager Elite or Kratos MALDI-IV) (*see* **Note 4**).
2. Determine the identity of trypsin-released fragments using the Protein Analysis Worksheet (PAWS, Macintosh version 6.0b2, copyright © 1995, Dr. Ronald Beavis—available on the Internet; *see* **Note 5**).

3.3. Results and Discussion

3.3.1. Protein Mass Mapping of a Protein–Protein Complex

The approach outlined in the Introduction has also been applied to protein-protein interactions, specifically to probe quaternary structure of cell cycle

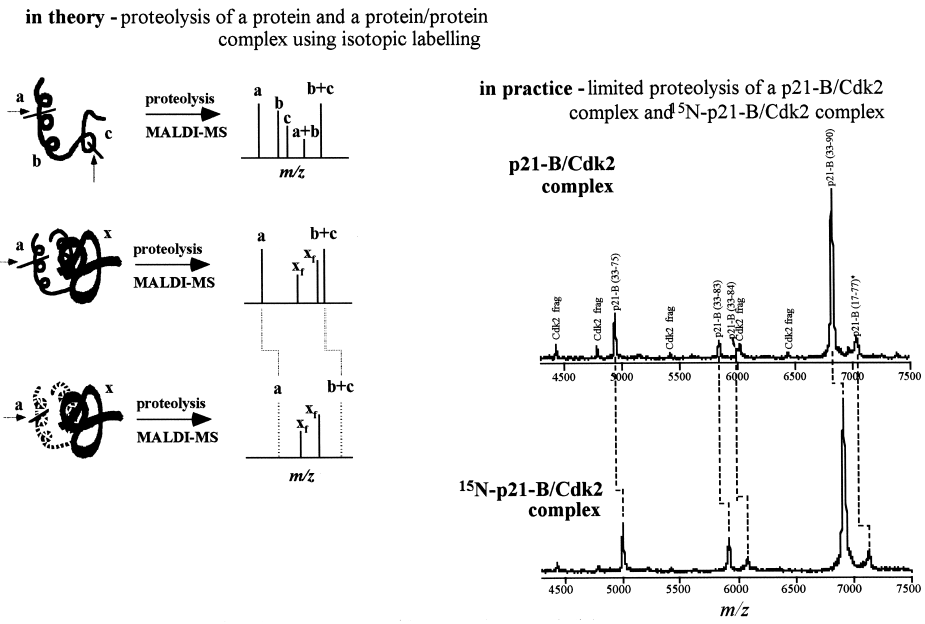

Fig. 2. Probing protein-protein interactions using proteolysis and MALDI-MS. Schematic view (left) of key concepts. Two cleavage sites are accessible for the protein of interest alone (top), yielding five fragments after limited digestion. In the complex with protein X, one site is protected (middle), yielding fewer fragments. However, fragments from protein X are also produced. Isotope labeling of the protein of interest causes fragments a and b+c to shift to higher *m/z* values, whereas fragments from protein X do not shift (bottom). Actual results are shown on the right.

Fig. 2 & 3

regulatory proteins, Cdk2 and p21$^{Waf1/Cip1/Sdi1}$ (**Figs. 2** and **3**) ***(4,5,9,12–21)***. A distinct and key advantage of this approach is that the masses of the fragments are obtained together in a *single* mass spectrum without the need for individual purification using, for example, HPLC or sodium dodecyl sulfate polyacrylamide gel electrophoresis (SDS-PAGE). Given a protein of known sequence and an enzyme with known sequence specificity, the mass usually identifies the exact fragment within the protein's sequence. The mapping of protein-protein complexes *in situ*, however, is complicated because peptide fragments are produced for all subunits within a complex.

We have recently demonstrated an alternative approach to mapping protein-protein interfaces that overcomes these complications ***(4,5)***. The experimental scheme, illustrated in **Fig. 2**, exploits the high mass accuracy, resolution, and sensitivity of MALDI-MS in combination with the power of stable isotope labeling. First, proteolysis reactions are performed for one component before

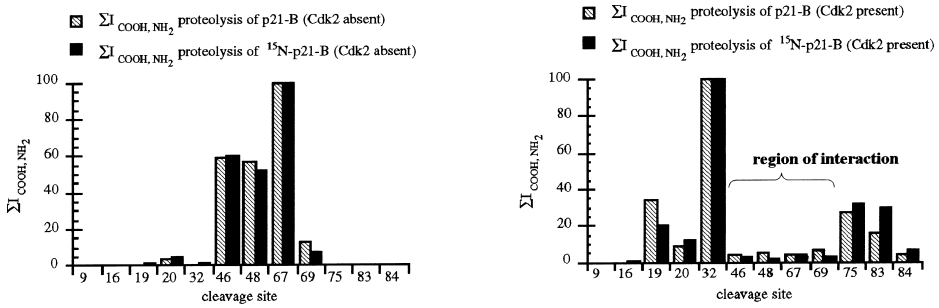

Fig. 3. Protected regions of p21-B within the p2l-B/Cdk2 complex. Trypsin accessibility at a particular cleavage site expressed as the sum of MALDI mass spectral peak intensities for all fragments with COOH- and NH_2-termini corresponding to scission at that particular site ($\Sigma I_{COOH,NH2}$), vs. position within the primary amino acid sequence (numbered with respect to the full-length p21 sequence). The left bar graph shows digestion results in the absence of Cdk2, and the right bar graph shows those in the presence of Cdk2. Results are given for natural isotopic abundance p2l-B **(hatched bars)** and 15N-p21-B **(solid bars)**.

and after formation of a multiprotein assembly (**Fig. 2**, left, top and middle). Proteolysis reactions for the complex are then performed in duplicate, with one subunit prepared at natural isotopic abundance in one experiment and in isotope labeled form in a second. Other proteins within the assembly are used at natural isotopic abundance in both experiments. Reaction products for both experiments are analyzed using MALDI-MS. **Figure 2** (right) clearly illustrates the power of isotope labeling in identifying peaks in spectra from digests of multiprotein assemblies; one subset of peaks occurs at shifted positions in the upper spectrum, whereas another subset does not. The former group of peaks arises from the isotope-labeled component of the assembly.

The mass accuracy of current-day MALDI-MS instruments (0.005%) allows reliable identification of most fragments from both p21 and CdK2 without resorting to isotope labeling. In these experiments, the kinase inhibitory domain of p21, called p21-B, was used. However, even this level of accuracy will not allow identification in all cases due to the finite probability that fragments from the different subunits will have similar masses. Therefore, separate p21-B samples were prepared with natural isotopic abundance and ^{15}N-labeled to allow for unambiguous differentiation of p21-B and Cdk2 fragments.

The results obtained from the protein mass mapping experiments on the p21-B/Cdk2 complex are summarized in the two bar graphs shown in **Fig. 3**. MALDI analysis of the tryptic fragments of p21-B, generated in the absence of Cdk2, was performed. The right-hand bar graph shows data after proteolysis of the p21/Cdk2 complex, with p21 at natural abundance (black) and ^{15}N-labeled

(gray). Cdk2 is unlabeled in both cases. These data revealed a segment of 24 amino acids in p21-B that is protected from trypsin cleavage, thus identifying the segment as the Cdk2 binding site on p21-B.

For proteins of known and potentially of unknown sequence, the protein mass mapping technique offers access to detailed information with only a modest investment in time and material. The accuracy and speed of this approach surpasses traditional methods based on HPLC/SDS-PAGE analysis and Edman degradation. Furthermore, due to the high resolution and sensitivity of MALDI mass analysis, a much greater number of protein fragments can be identified than was previously possible, offering more detailed "maps" of protein–protein structure. Based on the success of protein mass mapping with the DNA–protein and protein complexes, the MALDI method has recently been applied to the more highly structured and complex protein viral assemblies (*see* **Subheading 4.2.**) ***(22,23)***.

3.3.2. Time-Resolved Protein Mass Mapping of Viruses

Mass spectrometry has recently been recognized as a valuable source of information on both local and global viral structure ***(22–27)***. For instance, the mass measurement of viral capsid proteins is now straightforward and has even allowed the identification of posttranslational modifications ***(23,25,27)***. Since the viral capsids represent an interesting and important noncovalent quaternary association of protein subunits, viral analysis has been a logical step in the development of protein mass mapping. For instance, cleavage sites that reside on the exterior of the virus will be most accessible to the enzyme and therefore be among the first digestion fragments observed. Since proteolysis is performed in solution and can detect different conformers, this method can contribute to an understanding of the dynamic domains within the virus structure.

Virus particles are stable, yet exhibit highly dynamic character given the events that shape their life cycle. Isolated from their hosts, the nucleoprotein particles are macromolecules that can be crystallized and studied by X-ray diffraction. During assembly, maturation, and entry, however, they are highly dynamic and display remarkable plasticity. These dynamic properties can only be inferred from the X-ray structure and must be studied by methods that are sensitive to mobility.

Limited proteolysis/MALDI-MS experiments have been performed on human rhinovirus 14 (HRV14) and flock house virus (FHV). Virus HRV14, a causative agent of the common cold, is a member of a family of animal viruses called the picornaviruses, whose other members include the polio, hepatitis A, and foot-and-mouth disease viruses. The HRV14 virion consists of an icosahedral protein shell, or viral capsid, surrounding an RNA core. The capsid is composed of 60 copies of each of four structural proteins, VP1-VP4. Based on

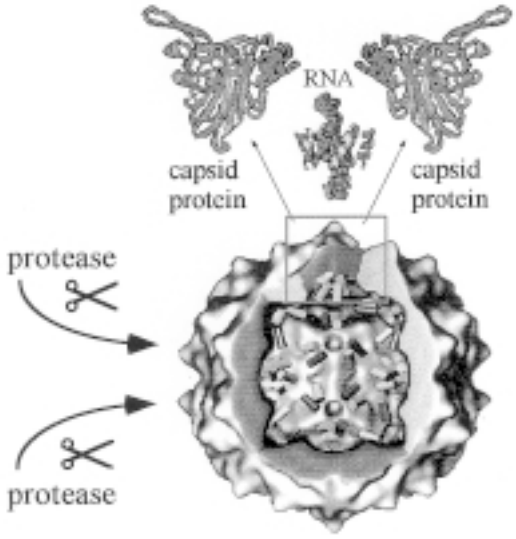

Fig 4. A nonenveloped icosahedral virus with a portion of the capsid proteins and RNA magnified above the virus. The experiments performed involved exposing viruses to limited proteolysis followed by mass analysis of the proteolytic fragments. Time-resolved proteolysis allowed for the study of protein capsid mobility. This encapsulated RNA virus (FHV) belongs to a structural class that includes thousands of viruses responsible for plant and animal diseases such as polio and the common cold.

crystal structure data ***(28)***, VP1, VP2, and VP3 compose the viral surface, whereas VP4 lies in the interior at the capsid-RNA interface. Virus FHV, like HRV14, is also a nonenveloped, icosahedral, RNA animal virus. The mature protein coat or capsid is composed of 180 copies of β-protein and γ-peptide (**Fig. 4**).

Fig. 4

Using time-resolved proteolysis followed by MALDI-MS analysis, it was expected that the reactivities of virus particles to different proteases would reveal the surface-accessible regions of the viral capsid and offer a new way of mapping the viral surface. In these studies, identification of the viral capsid protein fragments was facilitated by sequential digestion, in which proteins were first digested by an endoprotease, such as trypsin, and then exposed to an exoprotease such as carboxypeptidase ***(22,23)***. When these experiments were performed on both HRV ***(23)*** and FHV ***(22)***, cleavages on the surface-accessible regions were generated; however, cleavages internal to the viral capsids (based on the crystal structures) were also generated. Observation of digestion fragments resulting from internal protein regions was initially perplexing. After further examination, these results, along with the X-ray data, indicated that

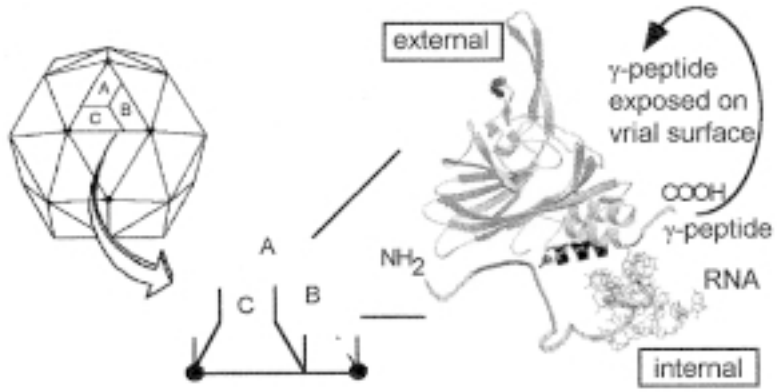

Fig 5. Crystal structure of Flock House virus shows that the γ-peptide and the N- and C termini of β-protein are localized internal to the virus. Yet, proteolytic time-course experiments demonstrated that these domains are transiently exposed on the viral surface.

portions of the internal proteins are transiently exposed on the surface of the virus (**Fig. 5**).

Fig. 5

The effects of drug binding on the viral capsid dynamics was also examined by protein mass mapping. Enzymatic digestions were performed in the presence of the antiviral agent WIN 52084 ***(23)***. The X-ray crystal structure of HRV14 reveals a 25-Å deep canyon on the surface of the virion at each five-fold axis of symmetry that has been identified as the site of cell surface receptor attachment. WIN compounds bind to these hydrophobic pockets, which lie beneath the canyon floor. Previous studies have shown that the binding of WIN compounds blocks cell attachment of some rhinovirus serotypes, inhibits the uncoating process, and stabilizes the viral capsid to thermal and acid inactivation.

MALDI-MS analysis of the virus following digestion in the presence of the WIN 52084 drug was significantly retarded after exposure to the enzyme for 3 h (**Fig. 6**) and even after 18 h, only two digestion fragments were observed. In control studies, mass mapping of other proteins and viruses in the presence of WIN 52084 revealed no inhibition of viral capsid degradation. Based on these results, it was concluded that WIN inhibition of protease activity was due to specific effects on the availability of HRV14 cleavage sites and not on the protease itself. The WIN drug is thought to inhibit the capsid mobility, thereby effecting the digestion of the virus.

Fig. 6

The protein mass mapping experiments offer a complementary approach to the inherently static methods of crystallography and electron microscopy and reveal dynamic structural changes in solution that may fundamentally alter the

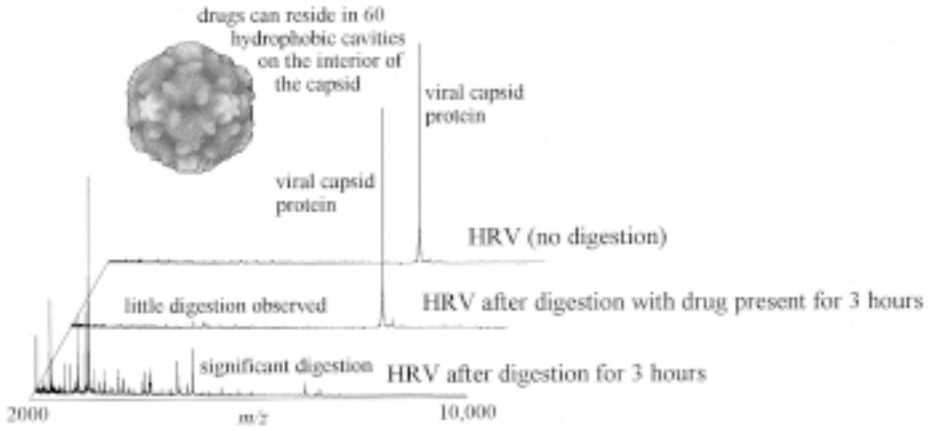

Fig 6. Inhibition of dynamics with drug present. MALDI-MS analyses were performed on HRV, HRV following proteolysis with drug present, and HRV following proteolysis. Inset is an electron micrograph of HRV. (Inset adapted from ref. ***29***.)

way we look at viruses. However, these observations are consistent with the events that shape the viral life cycle (cell attachment, cell entry, and nucleic acid release), a life cycle that demands a highly mobile viral surface.

3.3.3. Conclusions and Future Directions

In this era of the bioinformation revolution, biologic scientists are in a position to obtain information on intermolecular interactions without the need for site-directed mutagenesis and free of the caveats associated with that technique. Clearly, the examples presented in this chapter illustrate the utility of combining proteolysis and mass spectrometric analysis in structural studies of proteins and multicomponent protein-based assemblies. Because the mass spectrometry component of the experiments still requires sophisticated instrumentation and the computer analysis of mapping data requires chemical knowledge of underlying cleavage and modification reactions, these approaches currently remain in the realm of scientists experienced with these methods, such as those working in support laboratories. Importantly, however, the key concepts of the methods, as illustrated here, are simple, and the probing reactions are also simple to perform. In essence, these methods are within reach of the entire biologic community.

Beyond the methods discussed herein, what are the future directions and potential for mass spectrometry-based proteolytic mapping methods? Although current mass spectrometric instrumentation is limited by low resolution and low accuracy at the upper mass limits, indirect mass analysis (in which only the products of probing reactions rather than whole molecular assemblies need

be transmitted through the mass spectrometer) makes the window of opportunity quite broad indeed. We have discussed applications to biomolecular assemblies that have been conducted both with and without high-resolution structural data. In the early stages of structural studies, mass spectrometry-based probing methods are particularly well suited to provide rapid access to low-resolution maps that can then be used to guide subsequent high-resolution studies. However, this early stage may itself be an end-point in some investigations in which the simple identification of interacting residues is the desired information. As a complement to high-resolution structural information (either from X-ray crystallography or NMR spectroscopy), probing studies have already been shown to provide valuable and startling insights into protein structural dynamics and rearrangements. These investigations mark the take-off point for follow-up studies that seek to quantitate molecular parameters related to the kinetics and thermodynamics of the underlying dynamic phenomena. We are all familiar with the prominence of gel electrophoresis methods in molecular biology studies; we posit that mass spectrometry methods will capture this position as a primary research tool in coming years due to its superior sensitivity, precision, accuracy, and throughput. The applications discussed here are just a few examples of current approaches that will see expanded use in the future. Only time will tell what others will be invented.

4. Notes

1. Spectra shown are typically an average of spectra from 128 laser pulses.
2. See ref. ***21*** for preparation of HRV14.
3. The activity of all the enzymes was verified with control peptides.
4. MALDI-MS mass analysis of on-plate trypsin digestions was conducted using the PerSeptive Biosystems instrument.
5. External calibration typically was accurate to 0.05% and allowed unequivocal assignment of most proteolytic fragments.

Acknowledgments

The authors thank Jennifer Boydston for helpful editorial comments and Drs. Tom Steitz of (Yale University), Steve Reed (The Scripps Research Institute), Ludger Hengst (Max-Planck Institute, Martinsried, Germany), and Mark Watson (Scripps) for their insightful comments and helpful suggestions. This work was supported by grants from the NIH 1, R01 GM55775–01A1 and 1 S10 RR07273–01 (G.S.).

References

1. Fontana, A., Fassina, G., Vita, C., Dalzoppo, D., Zamai, M., and Zambonin, M. (1986) Correlation between sites of limited proteolysis and segmental mobility in thermolysin. *Biochemistry* **25,** 1847–1851.

2. Hubbard, S. J., Eisenmenger, F., and Thornton, J. M. (1994) Modeling studies of the change in conformation required for cleavage of limited proteolytic sites. *Protein Sci.* **3,** 757–768.
3. Edman, P. and Begg, G. (1967) A protein sequenator. *Eur. J. Biochem.* **1,** 80–91.
4. Kriwacki, R. W., Wu, J., Siuzdak, G., and Wright, P. E. (1996) Probing protein-protein interactions by mass spectrometry: analysis of the p21/Cdk2 complex. *J. Am. Chem. Soc.* **118,** 5320.
5. Kriwacki, R. W., Wu, J., Tennant, T., Wright, P. E., and Siuzdak, G. (1997) Probing protein structure using biochemical and biophysical methods: proteolysis, MALDI mass analysis, HPLC, and gel-filtration chromatography of p21Waf1/Cip1/Sdil. *J. Chromatogr.* **777,** 23–30.
6. Fontana, A., Zambonin, M., Polverino de Laureto, P., De Filippis, V., Clementi, A., and Scaramella, E. (1997) Probing the conformational state of apomyoglobin by limited proteolysis. *J. Mol. Biol.* **266,** 223–230.
7. Fontana, A., Polverino de Laureto, P., De Filippis, V., Scaramella, E., and Zambonin, M. (1997) Probing the partly folded states of proteins by limited proteolysis. *Fold Des.* **2,** R17–26.
8. Cohen, S. L., Ferre-D'Amare, A. R., Burley, S. K., and Chait, B. T. (1995) Probing the solution structure of the DNA-binding protein Max by a combination of proteolysis and mass spectrometry. *Protein Sci.* **4,** 1088–1099.
9. Kriwacki, R. W., Hengst, L., Tennant, L., Reed, S. I., and Wright, P. E. (1996) Structural studies of p21Waf1/Cip1/Sdil in the free and Cdk2-bound state: conformational disorder mediates binding diversity. *Proc. Natl. Acad. Sci. USA* **93,** 11,504–11,509.
10. Neidhardt, F. C., Bloch, P. F., and Smith, D. F. (1974) Culture medium for enterobacteria. *J. Bacteriol.* **119,** 736–747.
11. De Bondt, H. L., Rosenblatt, J., Jones, H. D., Morgan, D. O., and Kim, S. (1993) Crystal structure of cyclin-dependent kinase 2. *Nature* **363,** 595–602.
12. Harper, J. W., Adami, G. R., Wei, N., Keyomarsi, K., and Elledge, S. J. (1993) The p21 Cdk-interacting protein Cip1 is a potent inhibitor of G1 cyclin-dependent kinases. *Cell* **75,** 805.
13. El-Deiry, W. S., Tokino, T., Velculescu, V. E., Levy, D. B., Lin, D., Mercer, W. E., et al. (1993) WAF1, a potential mediator of p53 tumor suppression. *Cell* **75,** 817–825.
14. Toyoshima, H. and Hunter, T. (1994) p27, a novel inhibitor of G1 cyclin-Cdk protein kinase activity, is related to p21. *Cell* **78,** 67–74.
15. Polyak, K., Lee, M., Erdjument-Bromage, H., Koff, A., Roberts, J. M., Tempst, P., et al. (1994) Cloning of p27Kip1, a cyclin-dependent kinase inhibitor and a potential mediator of extracellular antimitogenic signals. *Cell* **78,** 59–66.
16. Lee, M.-H., Reynisdottir, I., and Massagué, J. (1995) Cloning of p57KIP2, a cyclin-dependent kinase inhibitor with unique domain structure and tissue distribution. *Genes and Dev.* **9,** 639–649.
17. Matsuoka, S., Edwards, M. C., Bai, C., Parker, S., Zhang, P. B., A., Harper, W. J., and Elledge, S. (1995) p57KIP2, a structurally distinct member of the

p21CIP1 Cdk inhibitor family, is a candidate tumor suppressor gene. *Genes Dev.* **9,** 650–662.

18. Nakanishi, M., Robetorye, R. S., Adami, G. R., Pereira-Smith, O. M., and Smith, J. R. (1995) Identification of the active region of the DNA synthesis inhibitory gene p21Sdil/CIP1/WAF1. *EMBO J.* **14,** 555–563.
19. Chen, J., Jackson, P. K., Kirschner, M. W., and Dutta, A. (1995) Separate domains of p21 involved in the inhibition of Cdk kinase and PCNA. *Nature* **374,** 386–388.
20. Luo, Y., Hurwitz, J., and Massagué, J. (1995) Cell-cycle inhibition by independent CDK and PCNA binding domains in p21Cip1. *Nature* **375,** 159–161.
21. Russo, A. A., Jeffrey, P. D., Patten, A. K., Massague, J., and Pavletich, N. P. (1996) Crystal structure of the p27Kip1 cyclin-dependent-kinase inhibitor bound to the cyclin A-Cdk2 complex. *Nature* **382,** 325–331.
22. Bothner, B., Dong, X.-F., Bibbs, L., Johnson, J. E., and Siuzdak, G. (1998) Evidence of Viral Capsid Dynamics Using Limited Proteolysis and Mass Spectrometry. *J. Biol. Chem.* **273,** 673–676.
23. Lewis, J. K., Bothner, B., Smith, T. J., and Siuzdak, G. (1998) Antiviral Agent Blocks Breathing of Common Cold Virus. *Proc. Natl. Acad. Sci. USA* **95,** 6774–6778.
24. Siuzdak, G., Bothner, B., Yeager, M., Brugidou, C., Fauquet, C. M., Hoey, K., et al. (1996) Mass spectrometry and viral analysis. *Chem. Biol.* **3,** 45–48.
25. Siuzdak, G. (1998) Probing viruses with mass spectrometry. *J. Mass Spectrom.* **33,** 203–211.
26. Gorman, J. J., Ferguson, B. L., Speelman, D., and Mills, J. (1997) Determination of the disulfide bond arrangement of human respiratory syncytial virus attachment (G) protein by matrix-assisted laser desorption/ionization time-of-flight mass spectrometry. *Protein Sci.* **6,** 1308–1315.
27. Gorman, J. J. (1992) Mapping of post-translational modifications of viral proteins by mass spectrometry. *Trac-Trends Anal. Chem.* **11,** 96–105.
28. Rossmann, M. G., Smith, T. J., and Rueckert, R. R. (1993) The structure of human rhinovirus 14. *Structure* Intro Issue xxiv-xxv.
29. Spencero, S. M., Sgro, J. Y., Dryden, K. A., and Baker, M. L. *J. Struct. Biol.* **120,** 11–21.